22nd International Conference on
Harmonisation within Atmospheric Dispersion Modelling for Regulatory Purposes
10-14 June 2024, Pärnu, Estonia

SOURCE RECONSTRUCTION BASED ON INVERSE ATMOSPHERIC TRANSPORT MODELLING WITH DEPOSITION MEASUREMENTS

Stijn Van Leuven[1,2,3], Pieter De Meutter[1,2], Johan Camps[1], Piet Termonia[2 3] and Andy Delcloo[2,3]

[1]Belgian Nuclear Research Centre, Mol, Belgium
[2]Royal Meteorological Institute of Belgium, Brussels, Belgium
[3]Department of Physics and Astronomy, Ghent University, Ghent, Belgium

Abstract: The use of deposition measurements as a tool in inverse modelling is assessed by applying the technique to the case of an undisclosed large release of ^{106}Ru in Eurasia during the autumn of 2017. The atmospheric transport model utilized for this investigation is FLEXPART, which is used to calculate the source-receptor sensitivities in backwards-in-time mode. Inverse modelling is performed with the inverse modelling tool FREAR, which has been amended to be compatible with deposition measurements as part of this work. A twin-experiment based on the ^{106}Ru release is implemented. Here the atmospheric transport model is ran in forward mode to generate synthetic observations, circumventing the impact of measurement and meteorological model errors. These synthetic observations are then used in Bayesian- and cost function-based inverse modelling schemes to reconstruct the initial source location.

***Key words:** Inverse modelling, wet & dry deposition, Ruthenium-106, twin-experiment, FLEXPART, FREAR*

INTRODUCTION

An accidental release of radioactive material into the atmosphere can present substantial health risks to the surrounding population. These health impacts depend upon a range of potentially unknown properties of the source, including its location, the release height, the quantity of radioactive material released, and the temporal variation of the release. Equipped with measurements and an atmospheric transport model (ATM), one can use inverse modelling techniques to reconstruct the unknown source term. Most often used for inverse modelling in this context are measurements of radionuclide air concentrations, as detected by different detector networks, whether on a regional or global scale. Less commonly used are measurements of dry and/or wet deposition. However, deposition measurements offer greater flexibility than air concentration measurements, as deposition collection tanks can quickly be placed in ad-hoc locations. Air concentration detectors, on the other hand, are typically part of a fixed sparse network of stations. A plume of radionuclides could in theory even pass unnoticed between two stations.

In this work, inverse modelling with deposition measurements is assessed by applying the technique to a twin-experiment of an undisclosed release of ^{106}Ru in Eurasia in 2017, hereafter referred to as the “Ruthenium case”. During October 2017 unusual amounts of ^{106}Ru were detected in most of Europe and other parts of the northern hemisphere (Masson et al., 2019). Air concentrations of >150 mBq m^{-3} and deposition values of >100 Bq m^{-2} were detected. While the detected amounts of radiation were harmless, they suggested a considerable release that could cause health effects nearby the point of release. Various measurements have been aggregated by Masson et al. (2019): more than 1,000 air concentration measurements and more than 100 deposition measurements. Inverse modelling based on the concentration measurements points to a source location in the southern Urals. The Federal State Unitary Enterprise “Production Association Mayak” in Ozersk, Russia (location shown in Figure 1) has been indicated as most consistent with the observations (Masson et al. 2019; Saunier et al. 2019). Only air concentration measurements were used directly to reconstruct the source in the former studies. In this work, inverse modelling with the use of deposition measurements will be studied.

METHODOLOGY

Inverse modelling

Inverse modelling of atmospheric transport and dispersion is most favourable with a linear atmospheric transport model, such as FLEXPART (Stohl et al., 2005; Pisso et al., 2019) which is used in this study. A linear ATM has field quantities y_i that scale linearly with the source term x_j:

$$y_i = \sum_j m_{ij} x_j \tag{1}$$

The proportionality factors m_{ij} are called the source receptor sensitivities (SRS). The relevant field quantities considered here are activity air concentration (expressed in, for example Bq m^{-3}) and deposition (expressed in, for example Bq m^{-2}). Each field has its own SRS values m_{ij}, which can theoretically be obtained by both forward- and backward-in-time calculations with FLEXPART (Seibert and Frank, 2004; Eckhardt et al., 2017). The advantage of a linear ATM is that the SRS values only need to be calculated once, allowing the generation of field values y_i for any source term x_j without the need to re-run the model. The general idea behind inverse modelling is then, given a set of observed field values o_i, to reconstruct the source term by finding the best fit of o_i to y_i by altering the source term x_j.

Two prominent inverse modelling techniques are a) Bayesian inference and b) cost function optimisation. Both techniques are implemented in the inverse modelling tool FREAR (De Meutter et al., 2018; De Meutter and Hoffman, 2020; De Meutter et al., 2024). The Bayesian method in FREAR uses a Gaussian likelihood and an inverse gamma distribution for the combined model and observation uncertainties. It takes into account detections, non-detections, misses and false alarms through the use of Currie detection limits. The cost function method is based on minimising a modified version of the geometric variance and also takes into account detections and non-detections.

Twin-experiments

So far FREAR has been able to work exclusively with air concentration measurements. For this work, the functionality of FREAR has been extended to also include wet and dry deposition measurements. The modified version of FREAR is let loose on the Ruthenium case by way of a twin-experiment. A twin-experiment consists of inverse modelling given a set of synthetic observations generated by a forward ATM calculation. For the source reconstruction we assume the true source location to be unknown. In that case, it is most efficient to compute the SRS values with backward-in-time simulations.

A twin-experiment removes measurement and meteorological uncertainties. Still, a perfect match to the synthetic observations is not necessarily expected for two reasons. Firstly, if the SRS values are obtained through backward-in-time calculations, technical differences in the ATM code will results in slightly different values compared to the forward-in-time calculation (Seibert and Frank, 2004; Eckhardt et al., 2017). Secondly, synthetic observations are generated by integrating the field values over multiple time-steps, leading to a loss of information. It is worth noting that this loss of information is fundamentally different between measurements of air concentration, dry deposition and of wet deposition due to their physical nature. Air concentration and dry deposition observations are made locally, and thus give information about the plume at that specific location. Wet deposition observations, on the other hand, contain radionuclides that were scavenged over the entire precipitating vertical. However, wet deposition can also potentially provide more temporal information. Whereas air concentration measurements are integrated over some time period (say, 24 hours), wet deposition is only collected in precipitating conditions that may only cover part of the observation window (say, tens of minutes). In this case, a wet deposition measurement would correspond to a higher temporal resolution compared to air concentration.

Synthetic observations are generated with a forward calculation, given the ^{106}Ru source term of Saunier et al. (2019). The deposition measurements aggregated by Masson et al. (2019) are reproduced from the forward calculation and used as synthetic observation for the twin-experiment. The deposition data used from Masson et al. (2019) was filtered based on time and location, and consists of 18 pure wet deposition measurements (rain water) and 13 total deposition measurements (wet and dry deposition). The locations of the two types of measurements are shown in Figure 1. In order to compare the loss of information for each type of measurement, 18+13=31 synthetic air concentration measurements are generated with the same observational parameters (i.e. location and timing) as the deposition measurements. In this way, a one-to-one comparison between the different types of measurements can be made. A total of five experiments are performed as part of the twin-experiment. These are inverse modelling based on the synthetic measurements of 1) wet deposition, 2) total deposition, 3) wet + total deposition, 4) air concentration and 5) wet + total deposition + air concentration. This numbering will further be used to refer to each experiment.

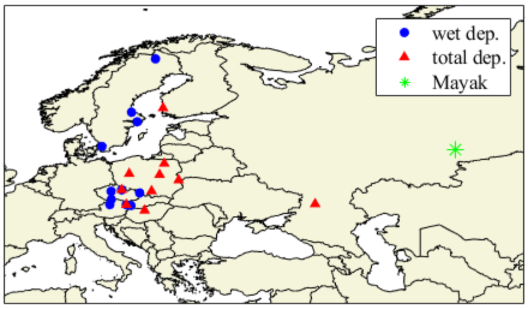

Figure 1. Locations of the 31 deposition measurements (blue dots: 18 wet deposition, red triangles: 13 total (wet + dry) deposition) selected from Masson et al. (2019). Some measurement locations overlap. Green star: location of the Mayak nuclear installation.

RESULTS

Figure 2 shows the source localisation using the cost function and Bayesian inference methods, comparing all five twin-experiments. The Bayesian method gives a probability map, while the cost function method shows the value of the minimised cost for each grid-box, which can be interpreted as a measure for the probability. For every experiment, both methods are able to correctly appoint a region of maximal probability to or very near to the true source location. However, the various experiments show significant differences in the fraction excluded from the domain.

The minimised cost of the deposition measurements (experiments 1, 2 and 3) exclude similar fractions of the domain. However, the total deposition experiment (2) provides a larger area of minimal cost compared to the wet deposition experiment (1). The combination of both (3) provides a smaller area still. These experiments also show local minima in cost to the west and west-south-west at several hundred and around a thousand kilometres from Mayak respectively. The air concentration experiment (4) is most fairly compared to experiment 3 (all deposition measurements) since these consist of the same measurement locations and observation windows. The cost function is able to pin-point the true source location extremely precisely. Further investigation reveals this is mostly explained by the fact that the ratios of synthetic concentration values to the (arbitrary, but realistic) minimal detectable quantity (MDQ) of 1 µBq m^{-3} are much higher compared to those of the deposition values (with an MDQ of 0.1 Bq m^{-2}). Due to the use of MDQ’s in the cost function (and Bayesian) method, values closer to and below the MDQ give the algorithm more freedom to fit the observations. Increasing the concentration MDQ to an unrealistically high value of 0.1 mBq m^{-3} results in a minimal cost region similar to that of experiment 3 (not shown). The combination of all deposition and concentration measurements (5) provides somewhat worse results than the concentration experiment (4), as new regions of low cost appear to the west and west-south-west, similar to those in the deposition experiments (1, 2 and 3). The region of lowest cost is still correctly appointed to the true source location, however.

The Bayesian inference method is able to exclude a much larger area of the domain for the deposition experiments (1, 2 and 3) compared to the cost function method. The wet deposition experiment (1) is localised more precisely than the total deposition measurement (2) in terms of both the maximal probability's distance to the true source and the fraction of the domain excluded. The combination of both types of deposition measurements (3) gives a comparable results to the wet deposition experiment (1). The concentration experiment (4) and all observations experiment (5), akin to the cost function method, are extremely accurate, thereby also affirming the fundamental correctness of the inverse modelling techniques.

CONCLUSIONS

Synthetic detections of the undisclosed release of radioactive ^{106}Ru in 2017 were used as a basis for a case study in source reconstruction with deposition measurements. This was done by setting up a twin-experiment, where synthetic detections were generated from a forward atmospheric transport calculation with a source term from the literature. From this, we conclude it is feasible to use deposition measurements for source localisation. The Bayesian inference method is able to exclude a larger fraction of the domain compared to the cost function optimisation method, as has been observed in previous studies using air concentration measurements. However, in practice meteorological and measurement uncertainties may mean a larger uncertainty is preferable. Source localisation with air concentration measurements gives much more precise results compared to the use of deposition. This is due to the fact that the ratios of observed values to minimal detectable values are much higher for the air concentrations than for the deposition. As part of future work, we will apply the techniques herein to the real deposition data available and also assess the optimised deposition parameters from Van Leuven et al. (2023).

REFERENCES

De Meutter, P., Camps, J., Delcloo, A. and Termonia, P., 2018: Source localisation and its uncertainty quantification after the third DPRK nuclear test: *Scientific Reports*, **8**.

De Meutter, P. and Hoffman, I., 2020: Bayesian source reconstruction of an anomalous Selenium-75 release at a nuclear research institute: *Journal of Environmental Radioactivity*, **218**.

De Meutter, P., Hoffman, I. and Delcloo, A. W., 2024: A baseline for source localisation using the inverse modelling tool FREAR: *Journal of Environmental Radioactivity*, **273**.

Eckhardt, S., Cassiani, M., Evangeliou, N., Sollum, E., Pisso, I. and Stohl, A., 2017: Source-receptor matrix calculation for deposited mass with the Lagrangian particle dispersion model FLEXPART v10.2 in backward mode: *Geoscientific Model Development*, **10**(12), 4605-4618.

Masson, O., Steinhauser, G., Zok, D., Saunier, O., Angelov, H., Babic, D., Beckova, V., Bieringer, J., Bruggeman, M., Burbidge, C. I., Conil, S., Dalheimer, A., Geer, L. E., Ott, A. D., Eleftheriadis, K., Estier, S., Fischer, H., Garavaglia, M. G., Leonarte, C. G., Zorko, B., 2019: Airborne concentrations and chemical considerations of radioactive ruthenium from an undeclared major nuclear release in 2017: *Proceedings of the National Academy of Sciences of the United States of America*, **116**(34), 16750-16759.

Pisso, I., Sollum, E., Grythe, H., Kristiansen, N. I., Cassiani, M., Eckhardt, S., Arnold, D., Morton, D., Thompson, R. L., Groot Zwaaftink, C. D., Evangeliou, N., Sodemann, H., Haimberger, L., Henne, S., Brunner, D., Burkhart, J. F., Fouilloux, A., Brioude, J., Philipp, A., . . . Stohl, A., 2019: The Lagrangian particle dispersion model FLEXPART version 10.4: *Geosci. Model Dev.*, **12**(12), 4955-4997.

Saunier, O., Didier, D., Mathieu, A., Masson, O. and Le Brazidec, J. D., 2019: Atmospheric modeling and source reconstruction of radioactive ruthenium from an undeclared major release in 2017: *Proceedings of the National Academy of Sciences of the United States of America*, **116**(50), 24991-25000.

Seibert, P. and Frank, A., 2004: Source-receptor matrix calculation with a Lagrangian particle dispersion model in backward mode: *Atmospheric Chemistry and Physics*, **4**, 51-63.

Stohl, A., Forster, C., Frank, A., Seibert, P. and Wotawa, G., 2005: Technical note: The Lagrangian particle dispersion model FLEXPART version 6.2: *Atmos. Chem. Phys.*, **5**(9), 2461-2474.

Van Leuven, S., De Meutter, P., Camps, J., Termonia, P. and Delcloo, A., 2023: An optimisation method to improve modelling of wet deposition in atmospheric transport models: applied to FLEXPART v10.4: *Geoscientific Model Development*, **16**(18), 5323-5338.

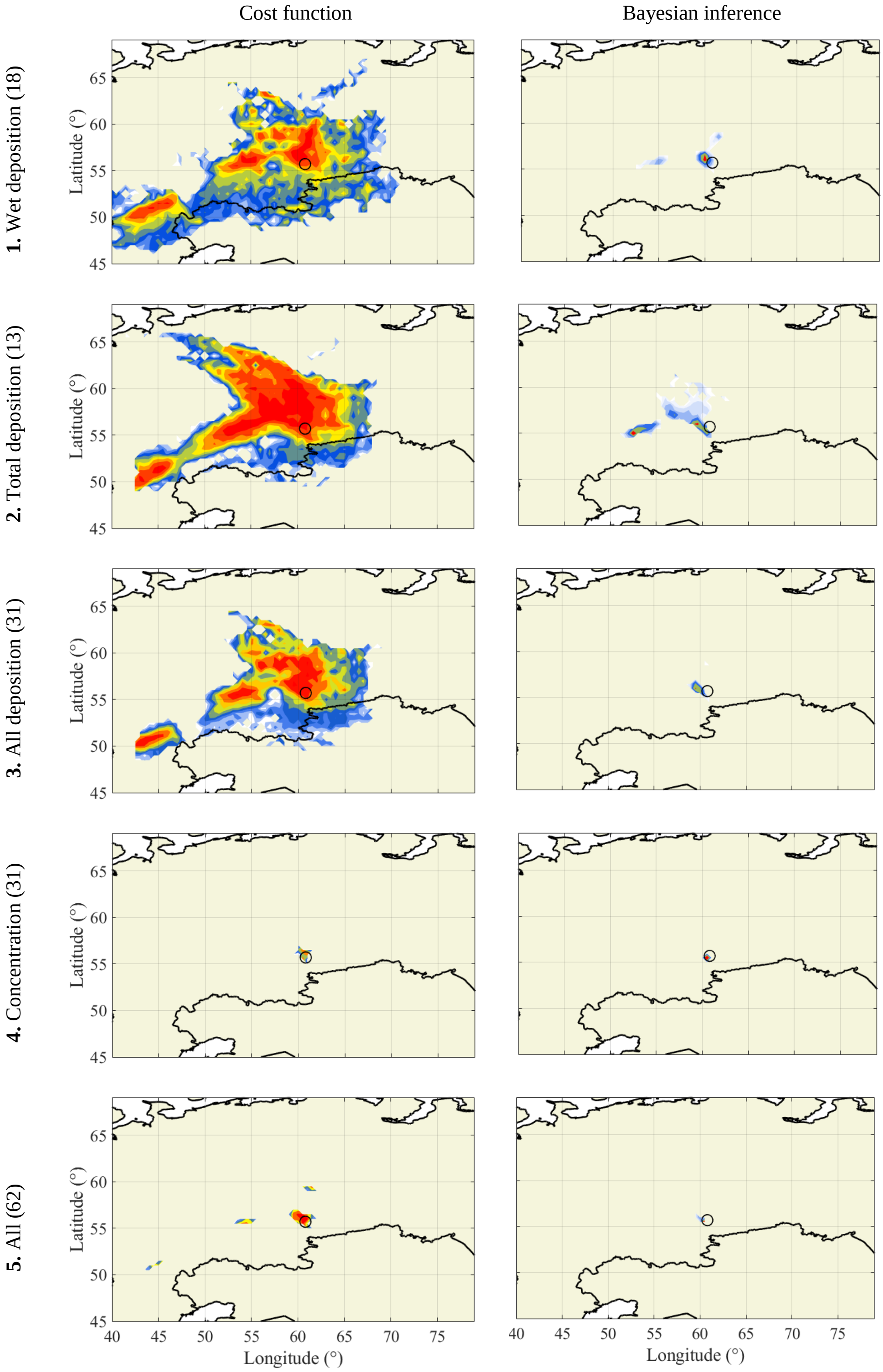

Figure 2. Source localisation for the five synthetic twin-experiments with cost function optimisation (red means lower cost) and Bayesian inference (red means higher probability). Black circle: location of the Mayak nuclear installation. In brackets are the number of measurements that are included in each experiment.